Nanotechnology **18** (2007) 445203 (5pp) doi:10.1088/0957-4484/18/44/445203

Operation of single-walled carbon nanotube as a radio-frequency single-electron transistor

Yong Tang[1], Islamshah Amlani[2], Alexei O Orlov[1], Gregory L Snider[1] and Patrick J Fay[1]

[1] Department of Electrical Engineering, University of Notre Dame, Notre Dame, IN 46556, USA
[2] Microelectronics and Physical Sciences Laboratory, Motorola Labs, Tempe, AZ 85284, USA

E-mail: ytang2@nd.edu

Received 8 August 2007, in final form 1 September 2007
Published 9 October 2007
Online at stacks.iop.org/Nano/18/445203

Abstract
We demonstrate the operation of a radio-frequency single-electron transistor (RF-SET) using single-wall carbon nanotubes (SWNTs). The device is embedded in a resonant tank circuit and operates in reflection mode at temperatures as high as 5 K. Both frequency domain and time domain results are presented. With a gate modulation frequency of 1 MHz, a charge sensitivity of $\sim 4.78 \times 10^{-4} e/\mathrm{Hz}^{-1/2}$ is obtained, which is limited by the large parasitic capacitance between the gate and the source/drain pads. Through the use of a top-gated configuration with reduced parasitic capacitance, both the RF performance and the charge sensitivity can be significantly improved.

1. Introduction

The radio-frequency single-electron transistor (RF-SET) is the most sensitive high-speed electrometer available for sub-electron charge detection. The operation of this device is based on loading a resonant RF tank (LC) circuit with an SET; the readout is performed by monitoring the change in the reflected [1] or transmitted [2] microwave power caused by changes in the charge on the gate electrode instead of directly measuring the change in the current or voltage in the SET. The major advantages of RF-SETs in comparison with conventional SETs for charge detection are the ability to measure sub-electron charges in a much wider bandwidth, and higher charge sensitivity than that of conventional SETs due to the reduction in $1/f$ noise in the detection bandwidth [1]. Since the first demonstration of an $\mathrm{Al/AlO}_x\mathrm{/Al}$ RF-SET [1], many applications of ultra-sensitive electrometers, such as read-out of quantum bits [3] and micromechanical displacement detectors [4], have been shown.

Carbon nanotube field-effect transistors (CNT FETs) are promising candidates for future electronic systems [5]. At low temperatures, CNT FETs typically exhibit single-electron tunneling behavior because the metal/carbon nanotube contacts form tunnel barriers with small ($\ll$1 fF) junction capacitances. Since the first observation of single-electron transport through ropes of carbon nanotubes by Bockrath *et al* [6] and later in individual CNTs by Tans *et al* [7], CNT-based SETs have shown several advantages over Al-based SETs. In particular, for CNT SETs, the area of the junctions and the volume of the quantum dot participating in Coulomb blockade are orders of magnitude smaller than in Al-based SETs, where the area of the junctions and the size of the quantum dot island are defined by the resolution of fabrication processing (typically electron-beam lithography). This improved scaling results in a high charging energy E_C (typically, $E_C > 2$ meV) and raises the operation temperature for CNT-based devices to $\sim$4 K or higher [8–10]. Based on the experimental configuration reported in [1], Roschier *et al* demonstrated the operation of RF-SETs based on multi-wall carbon nanotubes [11, 12] in a dilution refrigerator with a base temperature of 10 mK.

Here we demonstrate a single-walled carbon nanotube (SWNT) RF-SET that operates above liquid He temperatures ($\geqslant$5 K) and therefore does not require the use of sophisticated cryogenic equipment such as a dilution refrigerator for operation. Moreover, due to the higher operating temperature of these devices, the constraints on power dissipation are

much less strict. Consequently, larger RF carrier signal levels can be used, resulting in improved signal-to-noise ratio (SNR). With a carrier frequency of 336.737 MHz, a 1 MHz modulation signal is applied to the SET gate. The response of the CNT SET is detected in both the frequency and time domains. A charge sensitivity of $\delta q \approx 4.8 \times 10^{-4} e$ Hz$^{-1/2}$ has been achieved. The level of high-frequency sensitivity is limited in this device by parasitic capacitance between the back gate and the source–drain bonding pads. Despite this limitation, the device demonstrates promising RF response at a comparatively high working temperature and shows the potential for high charge sensitivity. These devices have potential uses as highly sensitive electrometers for the readout of charge configurations in advanced device architectures including quantum computing [3, 13, 14], quantum-dot cellular automata [15, 16], and also for real-time charge detection [17–19]. The high speed and high operational temperature of these devices promise to enable unprecedented performance in these systems without the complications associated with extremely low-temperature operation.

2. Experimental details

The SWNT SET was fabricated by the Embedded Systems Research group at Motorola Laboratories; the details of the fabrication process have been published previously [10]. In brief, Al/Ni bilayer catalyst islands are patterned on an oxidized silicon substrate using standard lithography and evaporation techniques followed by the growth of SWNTs in a chemical vapor deposition (CVD) chamber. The nanotube growth was performed at 800 °C and a pressure of 100 mTorr using methane (60 sccm) and hydrogen (40 sccm) source gases. Following nanotube growth, source and drain contacts are defined using standard photolithograpy and evaporation of Ti/Au metallization. A 2 μm separation between the two lithographically defined contacts defines the effective tube length. All of the processes used in the fabrication are compatible with conventional planar fabrication processing techniques. In operation, a highly doped Si substrate is used as a back-gate for the device. A schematic diagram of the completed device structure is shown in figure 1(a).

The measurement setup is shown in figure 1(b). The RF signal from a signal generator is split equally in two: one half is used to provide power to the local oscillator port of the mixer for homodyne detection, and the other half is attenuated and fed to the RF-SET through a directional coupler and bias tee. The signal reflected by the RF-SET is separated from the incident signal by the directional coupler and is amplified using a cryogenic (4.2 K) high electron mobility transistor (HEMT) pre-amplifier with a gain of 38 dB. The measurements are performed in a He cryostat in the temperature range 4.5–5 K.

The low-frequency conductance of the device is monitored using a lock-in technique, using a transimpedance amplifier connected to the SET's source contact to monitor the device current. To ensure the grounding of the device at high frequencies, the SET source is also shunted to ground through a 2000 pF chip bypass capacitor. At room temperature, the device shows decreasing conductance with increasing positive gate bias (with on-resistance of approximately

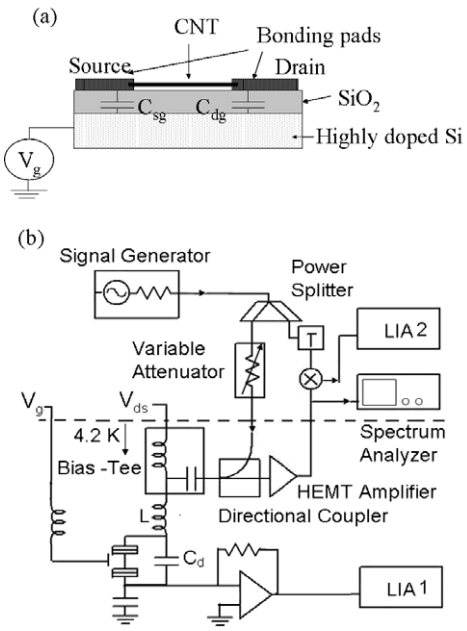

Figure 1. (a) Cross-section of the device showing parasitic capacitance between the back gate and the source/drain bonding pads. The thickness of SiO_2 is approximately 100 nm. (b) Schematic of the SWNT RF-SET measurement setup. The RF-SET is operated in reflection mode and both frequency domain and time domain setups are shown.

50 kΩ), indicating that the device is composed of a p-type semiconducting nanotube.

The charging diagram obtained at a temperature of 5 K, shown in figure 2(a), demonstrates single-electron transport with a charging energy of approximately 2 meV. This charging energy sets the upper limit on the operational temperature, $T \leqslant E_C/3k_B$, to be $\sim$7 K. We observe quasi-periodic oscillations with peaks of different heights, as shown in figure 2(b), which can result from either multiple quantum dots within the single CNT [10, 19–26], or possibly from a bundle of nanotubes between the source and drain contacts, resulting in parallel quantum dots.

To use this device as an RF-SET, the total capacitance from the drain to ground, C_d, is resonated with an external chip inductor to form a resonant tank circuit. A transmission line couples the incoming RF signal to the tank circuit. At resonance, the tank circuit transforms the parallel-connected nanotube impedance R_d from $\sim$100 kΩ to a much smaller impedance value $Z_T \approx L/(C_d R_d)$. Since the voltage reflection coefficient can be expressed as $\Gamma = \frac{Z_T - Z_0}{Z_T + Z_0}$, where $Z_0 = 50\ \Omega$ is the characteristic impedance of the transmission lines, a change of R_d due to charge modulation will cause a noticeable change in Γ due to the impedance transformation by the tank circuit.

For the device considered here, the parasitic capacitance between the drain and source bonding pads and the back gate, C_{dg} and C_{sg}, respectively, are treated as parallel-plate capacitors. Since the source and drain pads have identical geometries, we estimate $C_{dg} = C_{sg} = \varepsilon_0 \varepsilon \frac{S}{d} \approx 9$ pF, where S is the drain bonding pad area, $d = 100$ nm is the dielectric thickness and $\varepsilon = 3.9$ is the dielectric constant of

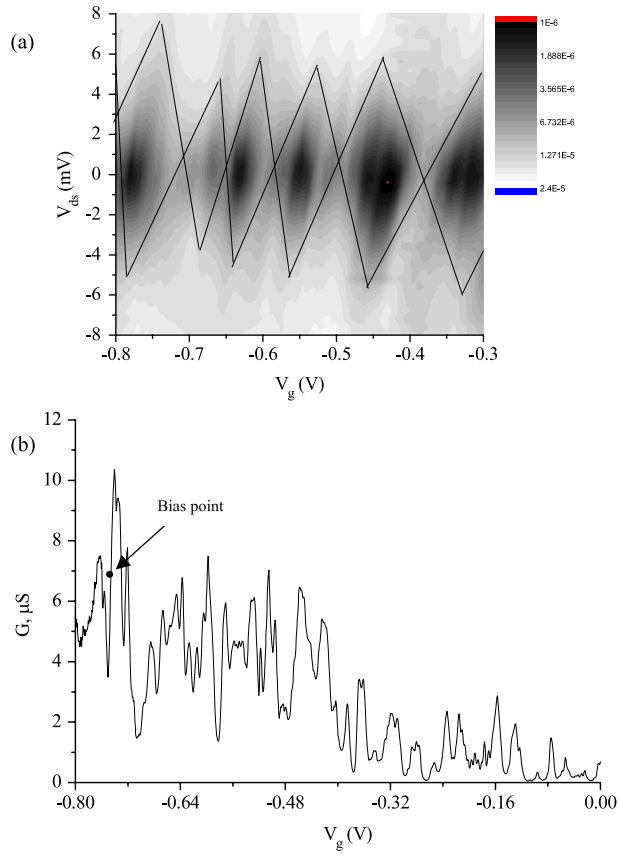

Figure 2. (a) Charging diagram of the CNT SET at $T = 5$ K, showing a charging energy $E_c \sim 2$ meV. (b) Gate dependence of Coulomb blockade oscillations at $T = 5$ K. Different peak heights and periods are likely due to either multiple quantum dots within the single CNT, or possibly from a bundle of nanotubes between the source and drain contacts, resulting in parallel quantum dots formed between the source and drain contacts. The smallest ΔV_m between adjacent conductance peaks is estimated to be 80.6 mV.

(This figure is in colour only in the electronic version)

SiO_2. We included an RF choke in series with the gate as shown in figure 1(b) to prevent the RF carrier signal applied to the drain from coupling into the external gate circuit. In this case the capacitance associated with the resonant tank circuit arises from the series interconnection of the drain-to-gate and gate-to-source capacitance. Thus the total tank capacitance is $C_d = (C_{sg}C_{dg})/(C_{sg} + C_{dg}) = C_{dg}/2 \approx 4.5$ pF. An external chip inductor of $L \sim 50$ nH is used to form the resonant tank circuit with designed resonant frequency of $f_0 = 1/2\pi\sqrt{LC_d} = 337.4$ MHz. The measured resonant frequency is $f_0 = 336.737$ MHz, close to the calculated value. Unfortunately, the high value of pad capacitance (compared to a typical values of 0.3–0.5 pF for implementations with Al-based RF-SETs [1–3, 27]) limits the gate modulation frequency response of the RF-SET, and therefore imposes a limit on the smallest resolvable signal at high frequencies. Another drawback caused by the large drain-to-gate capacitance is the signal coupling between the gate and the carrier signal path, which leads to the direct propagation of the gate signal into the drain circuit. This results in interference with the modulated carrier signal if it appears within the detection bandwidth. Both of these problems can be eliminated by using a top-gate configuration, with much reduced coupling between the source/drain and the gate. In a top-gate device, a larger resonator quality factor and increased resonant frequency could be achieved, resulting in higher charge sensitivity and wider detection bandwidth.

3. Results and discussion

The sensitivity of the SWNT RF-SET was determined using a high-frequency lock-in technique. The gate voltage is modulated with a sinusoidal signal $V_m\cos(\omega_m t)$, so

$$V_{bg} = V_{bg0} + V_m \cos(\omega_m t). \tag{1}$$

Assuming that the conductance of the device has a linear response at small modulation amplitudes V_m, both the conductance and reflection will be modulated at the same frequency:

$$G = G_0 + \frac{dG}{dV_{bg}} \times V_m \cos(\omega_m t) \tag{2}$$

$$\Gamma = \Gamma_0 + \frac{d\Gamma}{dV_{bg}} \times V_m \cos(\omega_m t), \tag{3}$$

where G_0 and $\Gamma_0 = (LG_0 - C_d Z_0)/(LG_0 + C_d Z_0)$ are the conductance and the reflection coefficient at V_{bg0}. Since the microwave carrier frequency is much larger than the modulation frequency, the reflected microwave signal can be written as

$$V_{refl} = V_c\Gamma\cos(\omega_c t) = V_c\left[\Gamma_0 + \frac{d\Gamma}{dV_{bg}} \times V_m \cos(\omega_m t)\right]\cos(\omega_c t), \tag{4}$$

where V_c is the carrier amplitude. With a non-zero Γ_0, the reflected signal is amplitude modulated by $d\Gamma/dV_{bg}$, which is proportional to the derivative of conductance dG/dV_{bg} or the slope of the Coulomb blockade oscillations. Mixing the reflected signal with the carrier signal, and using a lock-in amplifier to detect the demodulated signal at the output of the mixer, the dependence of dG/dV_{bg} versus V_{bg} can be recovered. Figure 3 shows a comparison of dG/dV_{bg} inferred from numerical derivative of the low-frequency conductance and that extracted from the microwave reflection measurement.

Measurement of the derivative of the conductance allows the minimum detectable signal, V_m, to be determined as a function of V_{bg}. Once the point of maximal charge sensitivity is determined, the SET is biased at that point (indicated by the arrow in figure 2(b)). An RF carrier power level of -60 dBm was chosen to maximize the derivative signal, which corresponds to a 632.5 μV_{pp} source–drain carrier signal.

With the SET biased at the operational point shown in figure 2(b), the smallest gate modulation signal that resulted in a detectable output was $V_m = 10.75\ \mu V_{pp}$. The minimum period of Coulomb blockade oscillations observed in figure 2(b) is $\Delta V_{bg}^{min} \approx 80.6$ mV. If we take this value as the oscillation period corresponding to one electron being added or removed from the dots formed within the CNTs, then the smallest detectable charge is given by [5]

$$\delta q_{rms} = \frac{V_m}{\Delta V_{bg}^{min}}\frac{e}{\sqrt{B}} \approx 4.78 \times 10^{-4} e/\mathrm{Hz}^{-1/2}, \tag{5}$$

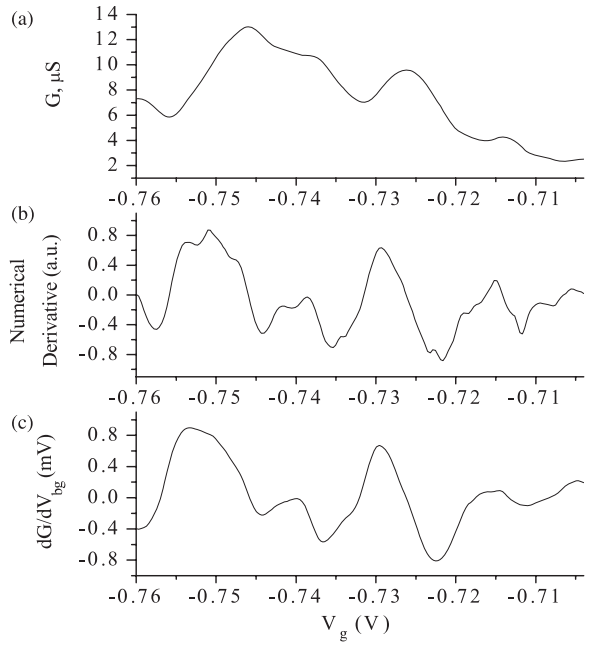

Figure 3. Derivative measurements demonstrating high-frequency operation of an SWNT SET. (a) Back-gate dependence of conductance. (b) Numerical derivative of $\mathrm{d}G/\mathrm{d}V_{\mathrm{bg}}$. (c) Detected $\mathrm{d}G/\mathrm{d}V_{\mathrm{bg}}$ using lock-in detection of the demodulated microwave reflection signal. The carrier frequency is 336.737 MHz and the gate modulation frequency is 1 MHz.

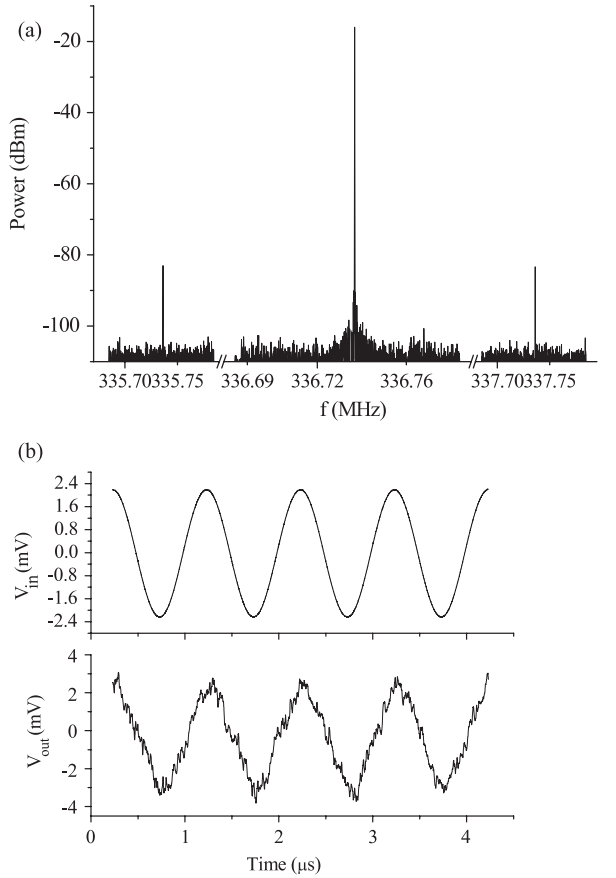

Figure 4. (a) Frequency spectrum of reflected signal with 4.52 $\mathrm{mV_{pp}}$ sine-wave gate modulation. The carrier frequency is 336.737 MHz and the gate modulation frequency is 1 MHz. The resolution bandwidth is 30 Hz. The tall central peak corresponds to the reflected carrier signal and the two side peaks correspond to the gate modulation. The SNR is the ratio between the side-peak height and the noise floor, approximately 20 dB. (b) Time domain response of an SWNT RF-SET with 4.48 $\mathrm{mV_{pp}}(0.055e_{\mathrm{pp}})$ sine-gate modulation at 1 MHz (top) and output curve (1648 trace average) (bottom).

where $B = 0.078$ Hz is the detection bandwidth of the lock-in amplifier and e is the electron charge.

The spectrum of the reflected signal shown in figure 4(a) was obtained by inspecting the reflected signal directly using an RF spectrum analyzer. A 4.52 $\mathrm{mV_{pp}}$ modulation signal was applied to the gate, resulting in two sidebands at $f_{\mathrm{c}} \pm f_{\mathrm{m}}$ (insets of figure 4(a)). Here the carrier frequency, f_{c}, is 336.737 MHz and the modulation frequency, f_{m}, is 1 MHz. Similarly, the rapid response of the RF SET in the time domain can be seen by examining the amplified output signal of the mixer on a digital oscilloscope. The average of 1648 individual traces, taken with a 1 MHz sine wave of amplitude 4.48 $\mathrm{mV_{pp}}$ applied to the gate, is shown in figure 4(b). The output shows a sine-wave response, demonstrating the high-frequency capability of the CNT SET.

4. Conclusions

We have demonstrated an RF-SET using single-walled carbon nanotube quantum dots. The SET operates at 5 K with a resonant frequency of 336.737 MHz and a modulation frequency of 1 MHz. Both frequency domain and time domain results are presented, and a charge sensitivity of $\delta q \approx 4.78 \times 10^{-4} e/\mathrm{Hz}^{-1/2}$ is estimated.

The large parasitic capacitance between the back gate and bonding pads due to the device geometry leads to compromised charge sensitivity. Furthermore, the direct propagation of the gate modulation signal into the RF carrier signal path limits the device performance for detection of non-sinusoidal modulating signals, as harmonic components of the signal can appear within the signal bandwidth. Such limitations can be eliminated by using a top-gate device structure with reduced parasitic gate–drain capacitance. The high working temperature and the high charge sensitivity of CNT-based SET devices will make them promising candidates in future nanotechnology.

Acknowledgments

We gratefully acknowledge support by the Keck Foundation, ONR, and NSF grant ECS-0100075.

References

[1] Schoelkopf R J, Wahlgren P, Kozhevnikov A A, Delsing P and Prober D E 1998 *Science* **280** 1238
[2] Fujisawa T and Hirayama Y 2000 *Japan. J. Appl. Phys.* **39** 2338
[3] Aassime A, Johansson G, Wendin G, Schoelkopf R J and Delsing P 2001 *Phys. Rev. Lett.* **86** 3376
[4] Blencowe M P and Wybourne M N 2000 *Appl. Phys. Lett.* **77** 3845

[5] Jing G, Hasan S, Javey A, Bosman G and Lundstrom M 2005 *IEEE Trans. Nanotechnol.* **4** 715
[6] Bockrath M, Cobden D H, McEuen P L, Chopra N G, Zettl A, Thess A and Smalley R E 1997 *Science* **275** 1922
[7] Tans S J, Devoret M H, Dai H, Thess A, Smalley R E, Geerligs L J and Dekker C 1997 *Nature* **386** 474
[8] Nygard J, Cobden D H, Bockrath M, McEuen P L and Lindelof P E 1999 *Appl. Phys.* A **69** 297
[9] Tans S J, Verschueren A R M and Dekker C 1998 *Nature* **393** 49
[10] Amlani I, Zhang R, Tresek J and Tsui R K 2004 *IEEE Trans. Nanotechnol.* **3** 202
[11] Roschier L, Sillanpaa M, Taihong W, Ahlskog M, Iijima S and Hakonen P 2004 *J. Low Temp. Phys.* **136** 465
[12] Roschier L, Hakonen P, Bladh K, Delsing P, Lehnert K W, Spietz L and Schoelkopf R J 2004 *J. Appl. Phys.* **95** 1274
[13] Shnirman A and Schon G 1998 *Phys. Rev.* B **57** 15400
[14] Fujisawa T, Hayashi T and Sasaki S 2006 *Rep. Prog. Phys.* **69** 759
[15] Orlov A O, Kummamuru R K, Ramasubramaniam R, Toth G, Lent C S, Bernstein G H and Snider G L 2001 *Appl. Phys. Lett.* **78** 1625
[16] Orlov A O, Kummamuru R K, Ramasubramaniam R, Lent C S, Bernstein G H and Snider G L 2003 *Surf. Sci.* **532** 1193
[17] Lu W, Ji Z, Pfeiffer L, West K W and Rimberg A J 2003 *Nature* **423** 422
[18] Bylander J, Duty T and Delsing P 2005 *Nature* **434** 361
[19] Biercuk M J, Reilly D J, Buehler T M, Chan V C, Chow J M, Clark R G and Marcus C M 2006 *Phys. Rev.* B **73** 201402
[20] Amlani I, Zhang R, Tresek J and Tsui R K 2003 *J. Vac. Sci. Technol.* B **21** 2848
[21] Li H, Zhang Q and Li J 2006 *Appl. Phys. Lett.* **88** 013508
[22] Matsumoto K, Kinoshita S, Gotoh Y, Kurachi K, Kamimura T, Maeda M, Sakamoto K, Kuwahara M, Atoda N and Awano Y 2003 *Japan. J. Appl. Phys.* **42** 2415
[23] McEuen P L, Bockrath M, Cobden D H, Yoon Y-G and Louie S G 1999 *Phys. Rev. Lett.* **83** 5098
[24] Postma H C, Teepen T, Yao Z, Grifoni M and Dekker C 2001 *Science* **293** 76
[25] Tsuya D, Suzuki M, Aoyagi Y and Ishibashi K 2005 *Japan. J. Appl. Phys.* **44** 2596
[26] Sapmaz S, Jarillo-Herrero P, Kouwenhoven L P and van der Zant S J H 2006 *Semicond. Sci. Technol.* **21** 52
[27] Bladh K, Gunnarsson D, Aassime A, Taslakov M, Schoelkopf R J and Delsing P 2003 *Physica* E **18** 91